Structure and Dynamic Behavior of Crowded Cis Vicinal [(*N*,*N*-Dimethylamino)cyclopentyl]trimethylammonium Salts and Related Compounds

Gideon Fraenkel,* Sharon Boyd, Albert Chow, and Judith Gallucci

Contribution from the Department of Chemistry, The Ohio State University, Columbus, Ohio 43210

Received July 8, 1996[⊗]

Abstract: Carbon-13 NMR spectra of [*cis*-2-(*N*,*N*-dimethylamino)cyclopentyl]trimethylammonium iodide (**4a**) and triflate (**4b**) in acetone-d_6 and in CD_3NO_2 show inversion of the amine with rotation about the ring−N bond to be unusually slow with $\Delta H^{\ddagger}$ and $\Delta S^{\ddagger}$ (**4b** in acetone-d_6) of 17 kcal/mol and 14 eu, similar to the values for *cis*-2-*tert*-butyl-1-(*N*,*N*-dimethylamino)cyclopentane (**3**) in Et_2O-d_{10} of 16 kcal/mol and 17 eu, indicating that steric and not electrostatic interactions are responsible for the slow rates. In addition, the N^+ methyls of **4a** and **4b**, which are magnetically nonequivalent by ^{13}C NMR at low temperatures, undergo signal averaging with increasing temperature, the result of rotation dynamics around the ring−N^+ bonds giving for **4b** in acetone-d_6 $\Delta H^{\ddagger}$ and $\Delta S^{\ddagger}$, respectively, of 7.2 kcal/mol and −9 eu. Similar values are found for *tert*-butyl rotation in **3** in Et_2O-d_{10}. Around room temperature for **4a** and **4b**, $^1J(^{14}N,^{13}C)$ is resolved and found to be ca. 3.6 Hz. With decreasing temperature, this coupling is averaged by progressively faster ^{14}N electric quadrupole induced relaxation. Line shape analysis of the ^{13}C NMR spectra shows E_a for the correlation time to be 2−2.7 kcal/mol. X-ray crystallography of **4b** and (*cis*-2-*tert*-butylcyclopentyl)trimethylammonium triflate (**7**) shows the rings to adopt the half-chair structure with vicinal substituents located at the puckered carbons. In **4b**, the N^+Me_3 group is pseudoequatorial with the NMe_2 group pseudoaxial; whereas, in **7**, the *tert*-butyl group is pseudoequatorial with the N^+Me_3 group pseudoaxial. Interesting correlations are noted of ^{13}C NMR shifts of individual methyls with their crystallographic structural assignments.

Cyclic cis vicinal diamines,[1] a hitherto neglected class of compounds due to the absence of an efficient preparation, are potentially useful as ligands for metal ions, are catalysts in the formation and reactions of organometallic compounds,[2] and show significant physiological activity. The Pt(II) complex of *cis*-1,2-diaminocyclohexane is an active anticancer agent.[3] Several substituted cis vicinal diaminocyclohexanes, for example (±)-*cis*-2-amino-4,5-dichloro-*N*-methyl-*N*-[2-(1-pyrrolidinyl)cyclohexyl]benzeneacetamide, were reported to bind to the σ receptor in the guinea pig brain.[4]

Our synthesis of cyclic cis vicinal tertiary diamines[5a,b] rendered these compounds readily accessible for the detailed study of their acid/base behavior and of their dynamics of conformational interconversion.[6] In the course of this work, we had occasion to prepare and investigate quaternary ammonium derivatives of these compounds. They displayed unusual dynamic behavior. This paper reports X-ray crystallographic studies and NMR investigations of dynamics in what now appear to be unusually crowded molecular species.

Results and Discussion

For convenience, the amines used in this work are listed as **1** to **3** together with their corresponding quaternary ammonium salts, **4**−**7**.

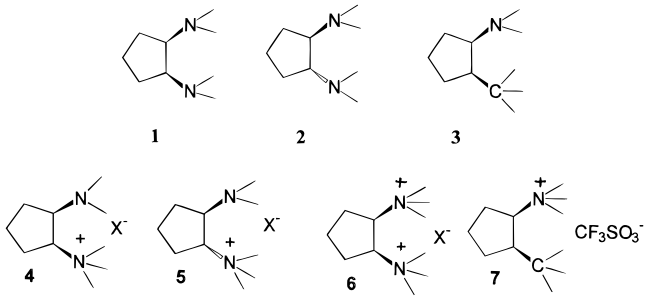

4a $X^- = I^-$ **5a** $X^- = I^-$ **6** $X^- = CF_3SO_3^-$
4b $X^- = CF_3SO_3^-$ **5b** $X^- = CF_3SO_3^-$
4c X^- = picrate

Of the compounds used in this work, *cis*-1,2-di(*N*,*N*-dimethylamino)cyclopentane (**1**) was prepared as described previously.[5,6] In parallel fashion, *cis*-2-*tert*-butyl-1-(*N*,*N*-dimethyl-

[⊗] Abstract published in *Advance ACS Abstracts,* December 1, 1996.

(1) (a) Confalone, P. N.; Pizzolato, G.; Uskokovic, M. R. *J. Org. Chem.* **1977**, *42*, 135−39. (b) Baker, B. R.; Anerry, M. V.; Safir, S. R.; Bernstein, S. *J. Org. Chem.* **1946**, *12*, 138−54. (c) Olsen, R. K.; Hennen, W. J.; Wardle, R. B. *J. Org. Chem.* **1982**, *47*, 4605−4611. (d) Parry, R. J.; Kunitani, M. G.; Vielle, O., III *J. Chem. Soc., Chem. Commun.* **1975**, 321. (e) Swift, G.; Swern, D. *J. Org. Chem.* **1967**, *32*, 511−517. (f) Confalone, P. N.; Pizzolato, G.; Baggiolini, E. G.; Lollar, D.; Uskokovic, M. R. *J. Am. Chem. Soc.* **1975**, *97*, 5936. (g) Mercuriamination: Barluenga, J.; Alonso-Cives, L.; Ansenio, G. *Synthesis* **1979**, 962−964. (h) Barluenga, J.; Aznar, F.; Liz, R. *J. Chem. Soc., Chem. Commun.* **1981**, 1181−1182. (i) Aminopalladation: Bäckvall, J. *Tetrahedron Lett.* **1978**, 163−166. (j) Chong, A. O.; Oshima, K.; Sharpless, K. B. *J. Am. Chem. Soc.* **1977**, *99*, 3420−3426. (k) Sharpless, K. B.; Singer, S. P. *J. Org. Chem.* **1976**, *41*, 2504−2506. (l) Levy, N.; Scaife, W.; Wilder-Smith, A. E. *J. Chem. Soc.* **1948**, 52−60. (m) Marx, M.; Marti, F.; Reisdorff, J.; Sandmeier, R.; Clark, S. *J. Am. Chem. Soc.* **1977**, *99*, 6754. (n) Broadbent, H. S.; Allred, E. L.; Pendleton, L.; Whittle, W. C. J. *J. Am. Chem. Soc.* **1960**, *82*, 189−93. (o) Becker, P. N.; White, M. A.; Bergman, R. G. *J. Am. Chem. Soc.* **1980**, *102*, 5676. (p) Kohn, H.; Jung, S. H. *J. Am. Chem. Soc.* **1983**, *105*, 4106. Jung, S. H.; Kohn, H. *J. Am. Chem. Soc.* **1985**, *107*, 2931. (q) Heine, H. G.; Fischler, H. M. *Chem. Ber.* **1972**, *105*, 975.

(2) For example, see: Langer, H. W. *Polyamine Chelated Alkali Metal Compounds*; Advances in Chemistry Series 130; American Chemical Society: Washington, DC, 1974; p 1.

(3) Gill, D. S.; Rosenberg, B. *J. Am. Chem. Soc.* **1982**, *104*, 4598.

(4) (a) DeCosta, B. R.; Redesca, L. *Heterocycles* **1990**, *31*, 1837. (b) DeCosta, B. R.; Bowen, W. D.; Hellewell, S. D.; George, C.; Rothman, R. B.; Reid, A. A.; Walker, J. M.; Jacobson, A. E.; Rice, K. C. *J. Med. Chem.* **1989**, *32*, 1996−2002.

S0002-7863(96)02327-X CCC: $12.00

Table 1. Quaternization of Amines

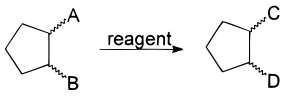

	A	B		reagent, solvent	C	D		
1	$N(CH_3)_2$	$N(CH_3)_2$	cis	CH_3I, Et_2O	$N(CH_3)_3{}^+I^-$	$N(CH_3)_2$	cis	**4a**
1	$N(CH_3)_2$	$N(CH_3)_2$	cis	$CF_3SO_3CH_3$, CH_2Cl_2	$N(CH_3)_3{}^+CF_3SO_3^-$	$N(CH_3)_2$	cis	**4b**
2	$N(CH_3)_2$	$N(CH_3)_2$	trans	CH_3I, Et_2O	$N(CH_3)_3{}^+I^-$	$N(CH_3)_2$	trans	**5a**
2	$N(CH_3)_2$	$N(CH_3)_2$	trans	$CF_3SO_3CH_3$, CH_2Cl_2	$N(CH_3)_3{}^+CF_3SO_3^-$	$N(CH_3)_3{}^+CF_3SO_3^-$	trans	**6**
4a	$N(CH_3)_2$	$N(CH_3)_3{}^+I^-$	cis	picric acid, Et_2O	$N(CH_3)_2$	$N(CH_3)_3{}^+$ picrate$^-$	cis	**4c**
3	$N(CH_3)_2$	$C(CH_3)_3$	cis	$CF_3SO_3CH_3$, CH_2Cl_2	$N(CH_3)_3{}^+CF_3SO_3^-$	$C(CH_3)_3$	cis	**7**

amino)cyclopentane (**3**) came from hydrogenation over Pd(C) of the enamine **9** obtained from 2-*tert*-butylcyclopentanone[7] (**8**).

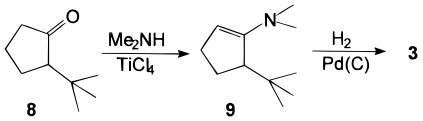

Compound **3** was assigned the cis structure on the basis that cyclic aminoenamines were already known to undergo catalytic hydrogenation on the unhindered side.[5] Subsequent X-ray crystallography of quaternary ammonium salt **7** confirmed the assignment (see below). *trans*-Diamine **2** was prepared by sodium in hot ethanol reduction of the *anti*-dioxine of cyclopentane-1,2-dione[8] followed by Eschweiler−Clark reductive alkylation of the resulting *trans*-1,2-diaminocyclopentane (**10**).

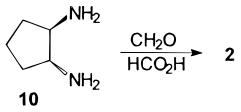

Formation of quaternary ammonium salts is summarized in Table 1. Alkylation of *cis*-diamine **1** using CH_3I, methyl triflate, or methyl picrate gave only monoquaternization (compound **4**). Repulsion between cis, N^+ substituents must render the corresponding transition state energetically inaccessible. However, with the nitrogens further apart, the *trans*-diammonium ditriflate **6** is rapidly formed and is stable.

Amines **1** and **3** were monoalkylated with methyl triflate as indicated in Table 1, and the resulting quaternary ammonium triflates **4b** and **7** were subjected to X-ray crystallography. The salient feature of these two structures is that the cyclopentane ring adopts the half-chair configuration with the vicinal substituents located on the puckered carbons (Figure 1 and 2). In **4b**, the trimethylammonium substituent is pseudoequatorial with the dimethylamino substituent pseudoaxial. Compound **7** has a similar arrangement with the *tert*-butyl pseudoequatorial and the trimethylammonium pseudoaxial. This is clearly seen by reference to the appropriate torsion angles (Table 2). The *tert*-butyl group of **7** and the trimethyl ammonium group of **4b** have torsion angles within the range of ±(165−180)° with respect to the unsubstituted ring carbons, whereas the corresponding values for the dimethylamine in **4b** and the trimethylammonium in **7** are 97.4(4)° and −99.0(6)°, respectively.

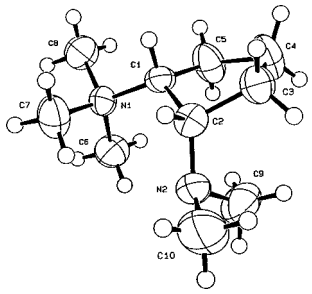

Figure 1. ORTEP drawing of **4b**. The non-hydrogen atoms are represented by 50% probability thermal ellipsoids. The hydrogen atoms are drawn with an artificial radius.

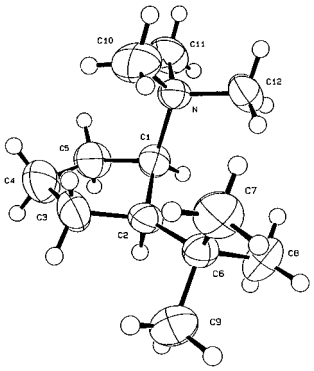

Figure 2. ORTEP drawing of **7**. The non-hydrogen atoms are represented by 50% probability thermal ellipsoids. The hydrogen atoms are drawn with an artificial radius.

Within the pseudoequatorial substituents, $N^+(CH_3)_3$ in **4b** and *tert*-butyl in **7**, one methyl group is sited perpendicular to the cyclopentane plane and the other two point away from the ring. This reduces hydrogen−hydrogen interactions. The bond to the pseudoaxial substituent nearly parallels the bond connecting the vertical methyl to the pseudoequatorial substituent.

The crystal structure of **4b** is also consistent with ^{13}C NMR data for **4b** in acetone-d_6. At low temperature, rotation around the ring−N^+ bond is slow enough to resolve three lines for the nonequivalent N^+ methyls (see below). One is unusually shielded with respect to the other two by 6−7 ppm and thus correlates with the perpendicular ammonium methyl seen with X-ray crystallography.

The structure of **4b** is similar to that of the monopicrate of *cis*-1,2-bis(dimethylamino)cyclopentane. X-ray crystallography showed the protonated nitrogen to be pseudoequatorial; the methyls point away from the ring with the NH^+ proton and picrate hydrogen-bonded to it, perpendicular to the three methylene carbon plane.[6]

Bond lengths and distances between groups indicate that the ring in **7** is larger and less symmetrical than that of **4b**. The average ring bond length in **4b** is 1.52 Å with a range of 1.588−1.511 Å, and in **7** it is 1.54 Å with a range of 1.588−1.527 Å.

(5) (a) Fraenkel, G.; Gallucci, J.; Rosenzweig, H. S. *J. Org. Chem.* **1989**, *54*, 677−681. (b) Previous procedures are summarized in cited refs 3−13 in ref 5a (given here). (c) Fraenkel, G.; Pramanik, P. *J. Org. Chem.* **1984**, *49*, 1314.

(6) Fraenkel, G.; Balasubramanian, V.; Chang, H. L.; Gallucci, J. *J. Am. Chem. Soc.* **1993**, *115*, 6795−6802.

(7) Chan, J. H.; Paterson, J.; Pinnsonnault, J. *Tetrahedron Lett.* **1977**, *48*, 4183.

(8) (a) Jaeger, F. M.; Blumendal, H. B. *Z. Anorg. Chem.* **1928**, 161. (b) Belcher, R.; Hoyle, W.; West, T. S. *J. Chem. Soc.* **1961**, 667. (c) Toftland, H.; Pederson, E. *Acta Chem. Scand.* **1972**, *26*, 4019.

Table 2. Selected Crystallographic Structural Parameters

	4a			**7**		
			Bond Length (Å)			
C(1)	C(2)	1.528(5)		C(1)	C(2)	1.588(7)
C(1)	C(5)	1.511(6)		C(1)	C(5)	1.533(8)
C(2)	C(3)	1.528(6)		C(2)	C(3)	1.527(8)
C(3)	C(4)	1.508(6)		C(3)	C(4)	1.528(9)
C(4)	C(5)	1.523(6)		C(4)	C(5)	1.548(10)
N(1)	C(1)	1.528(4)		N	C(1)	1.544(7)
N(2)	C(2)	1.457(5)		C(2)	C(6)	1.557(7)
			Bond Angles (deg)			
C(1)	C(2)	C(3)	100.6(3)	C(1)	C(2)	C(3)	104.7(4)
C(2)	C(3)	C(4)	100.0(4)	C(2)	C(3)	C(4)	105.7(5)
C(2)	C(1)	C(5)	100.9(3)	C(2)	C(1)	C(5)	100.5(4)
C(3)	C(4)	C(5)	107.2(4)	C(3)	C(4)	C(5)	106.3(5)
C(1)	C(5)	C(4)	103.6(4)	C(1)	C(5)	C(4)	108.5(5)
N(1)	C(1)	C(2)	118.5(3)	N	C(1)	C(2)	120.8(4)
N(2)	C(2)	C(1)	117.0(3)	C(1)	C(2)	C(6)	127.3(4)
			Torsion Angles (deg)			
N(1)	C(1)	C(2)	N(2) 44.3	N	C(1)	C(2)	C(6) −59.4(7)
N(2)	C(2)	C(3)	C(4) 97.4(4)	N	C(1)	C(5)	C(4) −99.0(6)
N(1)	C(1)	C(5)	C(4) 107.1(3)	C(4)	C(3)	C(2)	C(6) −179.4(5)

In the separation of the groups, the C1−C2 bond of **7** is 1.588(7) Å and that of **4b** is 1.528(8) Å. The length of the N1−C1 bond is 1.544(7) Å for **7** and 1.528(4) Å for **4b**. The C2−C6 bond is 1.557(7) Å, and the N2−C2 bond of **4b** is 1.457(5) Å. The distance between N1 and C6 of **7** is 3.558(7) Å, and the distance between N1 and N2 of **4b** is 3.085(5) Å.

The bond angles in Table 2 show the increased distortion of **7** due to the two bulky groups. In **7**, the N−C1−C2 angle is 120.8(4)° and the C1−C2−C6 angle is 127.3(4)°. For **4b**, the N1−C1−C2 angle is 118.5(3)° and the N2−C2−C1 angle is 117.0(3)°. The bond angles for the cyclopentyl ring are larger (∼2°) for **7** compared to those of **4b**. The positioning of the methyl groups is reflected in the bond angles. The $C_{ring}-N^+-CH_3$ angle in **4b** for the methyl sited over the ring is 114° while the other methyls are near the sp^3 hybridization angle with values of 108° and 109°.

In sum, the X-ray structures show that the cyclopentane rings distort to accommodate adjacent bulky groups.

The NMR data for compounds **3** to **7** displayed some unexpected correlations as well as detailed insight into the dynamic behavior of three particular species (**4a**, **4b**, and **3**).

At room temperature, ^{13}C NMR spectra of $N(CH_3)_2$ in **1**−**5** all show single lines with much the same shifts (see Table 3), apparently independent of electrostatic and steric effects. The series includes cis and trans vicinal diamines as well as cis and trans vicinal aminoammonium salts.

In compounds **4a** and **4b** at low temperature, ^{13}C NMR spectroscopy shows the $N(CH_3)_2$ methyls to be magnetically nonequivalent (see Figures 3 and 4), conditions under which the rates of inversion at nitrogen and rotation around the ring−$N(CH_3)_2$ bonds are slow relative to the NMR time scale. To see whether this behavior was unique to the proximity of a cis vicinal trimethylammonium substituent, the ^{13}C NMR of **3**, isoelectronic with the cation moiety of **4b**, was also obtained at low temperature (Figure 5). The $N(CH_3)_2$ ^{13}C NMR resonance of **3** behaved in similar fashion to those of **4a** and **4b**; hence, the line shape changes are of steric and not electrostatic origin. As seen in Table 4, the ^{13}C NMR shifts within each dimethylamino pair for **3**, **4a**, and **4b** are remarkably similar. One methyl at ca. δ 46 is quite similar to that in a "normal" acyclic environment; the other is shielded by ca. 7 ppm. This suggests that the structure of **3** is similar to that of **4b**, with the dimethylamino group being pseudoaxial with the shielded methyl at δ 38−39 directed over the cyclopentane moiety, by analogy to the X-ray crystallographic results.

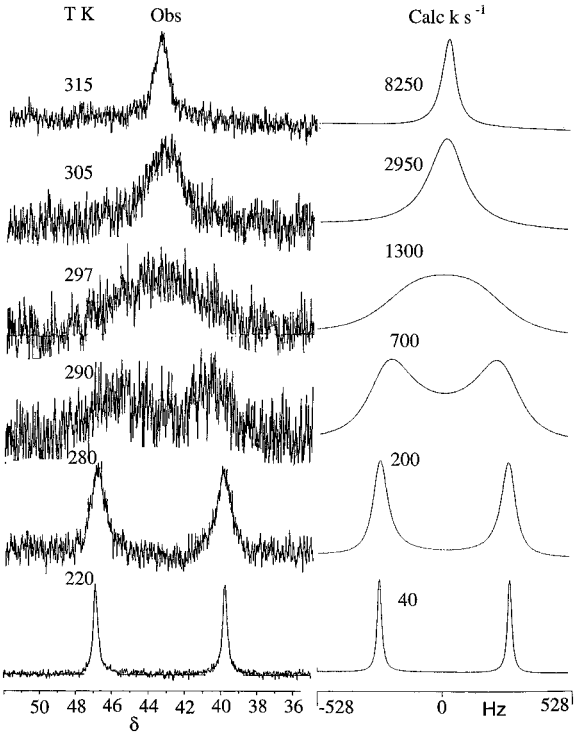

Figure 3. ^{13}C NMR compound **4a** in CD_3NO_2, $N(CH_3)_2$ part (left) observed at different temperatures and (right) calculated to fit with rate constants.

At room temperature all but one of the quaternary ammonium salts display spin coupling between the ^{14}N and the directly bonded ^{13}C of methyl of around 4 Hz (see Table 3), the

Table 3. ^{13}C NMR Shifts (δ) and $^1J(^{13}C,^{14}N)$ Values (Hz) for Amines and Salts (at 300 K)

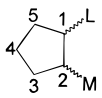

		L	M	1	2	3	4	5	L	M	$^1J(^{13}C,^{14}N)$
1[a]	cis	NMe_2	NMe_2	68.72	68.72	25.91	22.00	25.91	44.32	44.32	
2[a]	trans	NMe_2	NMe_2	69.97	69.97	26.75	24.32	26.75	42.99	42.99	
4a[b]	cis	$NMe_3^+I^-$	NMe_2	74.86	64.24	20.23	19.94	23.52	53.03	43.08	3.4
4b[b,d]	cis	$NMe_3^+CF_3SO_2^-$	NMe_2	74.88	64.12	19.95	19.64	23.06	52.14	43.15	3.4
5a[b]	trans	$NMe_3^+I^-$	NMe_2	76.82	66.28	22.18	20.34	26.24	52.53	40.99	3.9
6[b,d]	trans	$NMe_3^+CF_3SO_3^-$	$NMe_3^+CF_3SO_3^-$	77.36	77.36	29.01	25.59	29.01	52.93	52.93	
3[c]	cis	NMe_2	CMe_3	67.08	35.77	23.07	22.50	25.64	43.56	28.91	
7[b,d]	cis	$NMe_3^+CF_3SO_3^-$	CMe_3	80.23	56.21	25.08	19.98	26.60	53.92	32.03 30.46 32.01	3.4

[a] $CDCl_3$ solution. [b] Acetone-d_6. [c] Diethyl ether-d_{10}. [d] Triflate $^1J(^{13}C,^{19}F) = 320$ Hz.

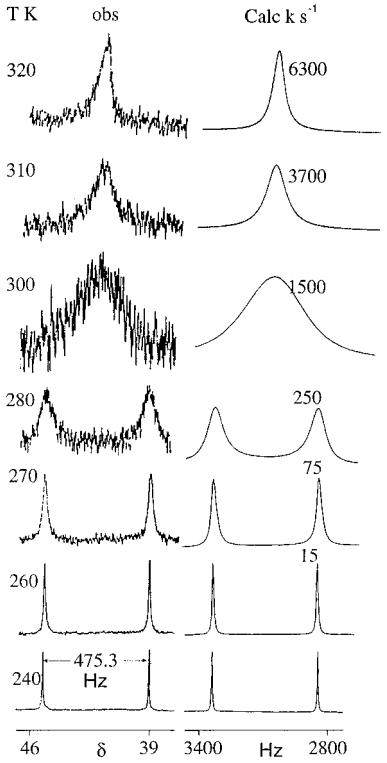

Figure 4. ^{13}C NMR compound **4b** in acetone-d_6, $N(CH_3)_2$ portion (left) observed at different temperatures and (right) calculated to fit with rate constants.

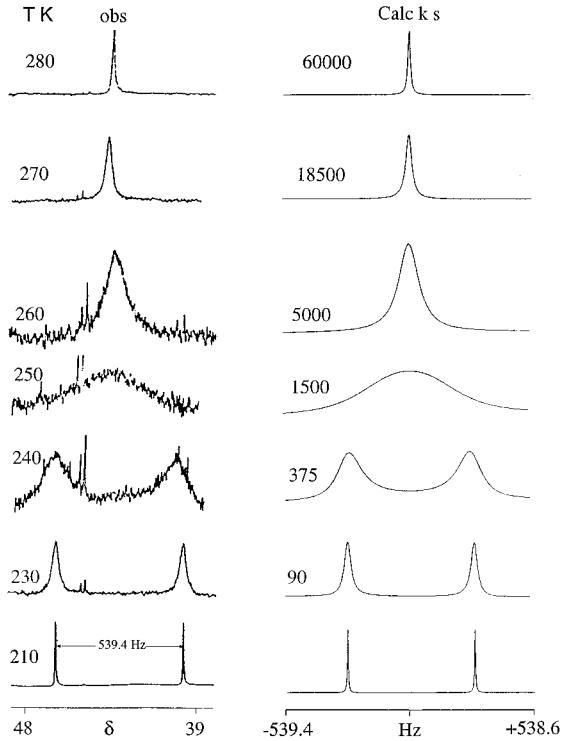

Figure 5. ^{13}C NMR compound **3** in diethyl ether-d_{10}, $N(CH_3)_2$ part (left) observed at different temperatures and (right) calculated line shapes, to fit with rate constants.

exception being the *trans*-1,2-diammonium salt **6**. Evidently, electric field gradients around the ^{14}N in these salts must be quite small compared to most ammonium salts wherein ^{14}N electric quadrupole-induced relaxation is fast enough to average $^1J(^{13}C,^{14}N)$. In addition to common values for the latter spin coupling, the ^{13}C NMR shifts for NCH_3^+ are similar for the ammonium salts. With decreasing temperature, the triplet

Table 4. Low Temperature ^{13}C NMR Chemical Shifts (δ) for *cis*-1-$N(CH_3)_2$-2-$X(CH_3)_3$-*c*-C_5H_8

	$X(CH_3)_3$			$X(CH_3)_3$	$N(CH_3)_2$	
3[a]	23.21	29.6	33.5	$C(CH_3)_3$	39.64	46.8
4a[a]	47.45	52.96	55.99	$N(CH_3)_3^+I^-$	39.15	46.36
4a[b]				$N(CH_3)_3^+I^-$	39.64	46.79
4b[a]	47.00	52.92	56.05	$N(CH_3)_3^+CF_3SO_3^-$	38.19	46.23

[a] Acetone-d_6. [b] Nitromethane-d_3.

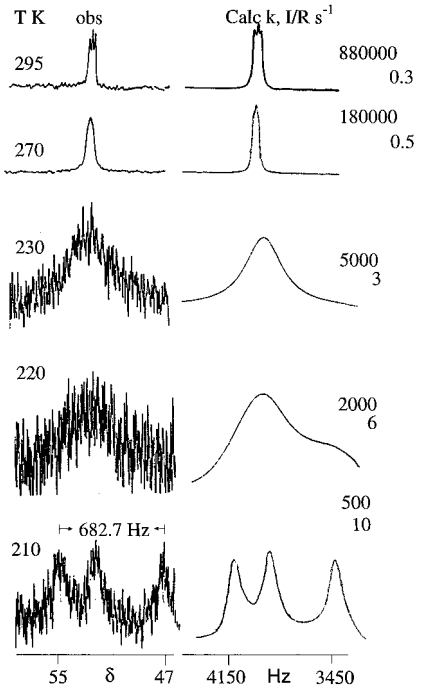

Figure 6. ^{13}C NMR compound **4a** in acetone-d_6, $N(CH_3)_3^+$ part (left) observed at different temperatures and (right) calculated to fit with rate constants for rotation and ^{14}N quadrupole-induced relaxation.

structure due to $^1J(^{13}C,^{14}N)$ in **4a** and **4b** in acetone-d_6 solution undergoes averaging, due to faster ^{14}N nuclear electric quadrupole-induced relaxation, followed by extensive broadening of the resonance and then by 200 K three lines of equal intensity resolve indicating that by this temperature rotation around the ring−N^+ bond has become slow relative to the NMR time scale (see Figures 6 and 7). The spacing of the three NCH_3^+ ^{13}C NMR resonances of **4a** and **4b** at low temperature is quite similar to that seen for the C methyls of *cis*-2-*tert*-butyl-1-(*N*,*N*-dimethylamino)cyclopentane (**3**) in Et_2O-d_{10} solution at 170 K (see Table 4). One can also conclude that the N^+ methyls in **4a** and **4b** and the C methyls in **3** must reside in similar environments; in each case, one methyl is shielded with respect to the other two in the group. This is consistent with the crystallographic finding that one of the ammonium methyls of **4b** is perpendicular to the three methylene carbon plane of the ring and the other two are pointing away from the ring (Figure 1). The significance of the N^+-CH_3 ^{13}C NMR data will be further discussed below.

NMR line shapes for the ^{13}C NMR resonances of the dimethylamino methyls were calculated as a function of the composite rate of inversion at nitrogen with rotation around the ring−N bond.[9] This resonance is treated as an uncoupled, equally populated, two half-spin exchanging system (eq 1), wherein the numbers label the spins (^{13}C) and X and Y stand for the two environments.[9] Comparison of experimental $N(CH_3)_2$

(9) (a) Gutowsky, H. S.; Saika, H. J. *J. Chem. Phys.* **1953**, *21*, 1688. (b) Gutowsky, H. S.; Holm, C. H. *Ibid.* **1957**, *25*, 1288. (c) Kaplan, J. I.; Fraenkel, G. *J. Am. Chem. Soc.* **1972**, *94*, 2907.

$$X_1Y_2 \rightleftarrows Y_1X_2 \qquad (1)$$

^{13}C NMR line shapes for compounds **4a**, **4b**, and **3** with the calculated line shapes, respectively, (Figures 6−8) provides the rate constants for inversion/rotation treated in, for example, the Eyring plot shown in Figure 9. Table 5 lists the associated activation parameters. The similarity of $\Delta H^{\ddagger}$ for **4a** and **4b** might have been expected; that their values resemble the barrier for **3** confirms the similarity of the N−$(CH_3)_2$ environments in all three species as proposed above and implies that the mechanisms for inversion/rotation must be similar and that steric effects are predominantly responsible for the large magnitude of the barriers rather than electrostatic interactions. Ordinarily in the absence of steric effects such barriers are much lower than those found in this work. For example, in *N*,*N*-dimethyl-*tert*-butylamine the value is 6 kcal/mol.[10]

Symbols used in the following NMR line shape calculations are conveniently collected in Table 6.

Carbon-13 NMR line shape changes for the *tert*-butyl methyls of **3** due to rotation around the *tert*-butyl ring bond are treated as an equally populated uncoupled three half-spin exchanging system (eq 2).[11]

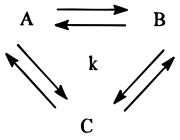

(2)

the absorption is given by the summation (eq 3)

$$\mathrm{Abs}(<) = -\mathrm{Im}(\rho^{A} + \rho^{B} + \rho^{C}) \qquad (3)$$

the ρ^{i} being abbreviations for the density matrix elements $\langle\beta|\rho^{i}|\infty\rangle$. The three latter elements are obtained by solving the three coupled density matrix equations, shown in matrix form (eq 4)

$$\begin{bmatrix} \mathrm{i}2\pi\Delta\nu_A - T^{-1} - 2k & k & k \\ k & i2\pi\Delta\nu_B - T^{-1} - 2k & k \\ k & k & \mathrm{i}2\pi\Delta\nu_C - T^{-1} - 2k \end{bmatrix} \begin{bmatrix} \rho^{A} \\ \rho^{B} \\ \rho^{C} \end{bmatrix} = \mathrm{i}C \begin{bmatrix} 1 \\ 1 \\ 1 \end{bmatrix} \qquad (4)$$

which were generated from the three elements of the density matrix equations $\dot{\rho}^{A}_{\beta,\alpha}$, and $\dot{\rho}^{B}_{\beta,\alpha}$, and $\dot{\rho}^{C}_{\beta\alpha}$, the first of which is shown in (eq 5),

$$\dot{\rho}^{A}_{\beta,\alpha} = \langle\beta|\mathrm{i}[\rho^{A},H^{A}] + T^{-1}\rho^{A} + k(\rho^{A}(\mathrm{ae}) - (\rho^{A})|\alpha\rangle \qquad (5)$$

with the symbols defined as in Table 6. The after exchange elements of the density matrix ρ^{i} are obtained by inspection of the exchange process (see for example an element of ρ^{A}(ae), eq 6).

$$\rho^{A}(\mathrm{ae}) = \rho^{B} + \rho^{C} \qquad (6)$$

Comparison of observed and calculated carbon $^{13}CH_3$ resonances of **3** (Figure 8, in diethyl ether-d_{10}) provided the rate constants for rotation and activation parameters $\Delta H^{\ddagger}$ and $\Delta S^{\ddagger}$ of 16 kcal/mol and 17 eu, respectively; Figure 10 is the Eyring plot (see Table 5).

Analysis of the trimethylammonium ^{13}C NMR line shapes is a little more complicated than that above, since account must also be taken of $^{1}J(^{13}C,^{14}N)$ in **4a** and **4b** and its averaging due

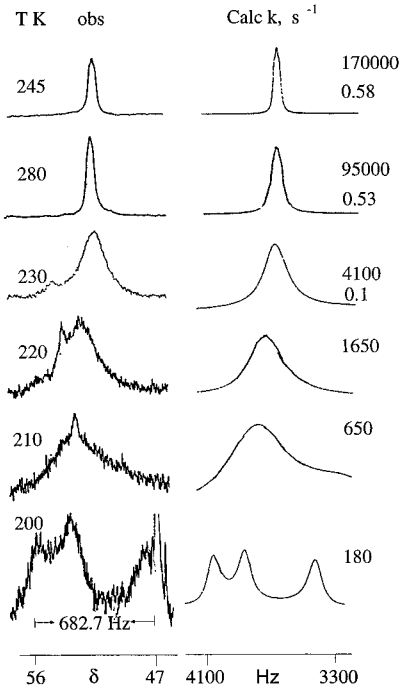

Figure 7. ^{13}C NMR compound **4b** in acetone-d_6 as in Figure 6.

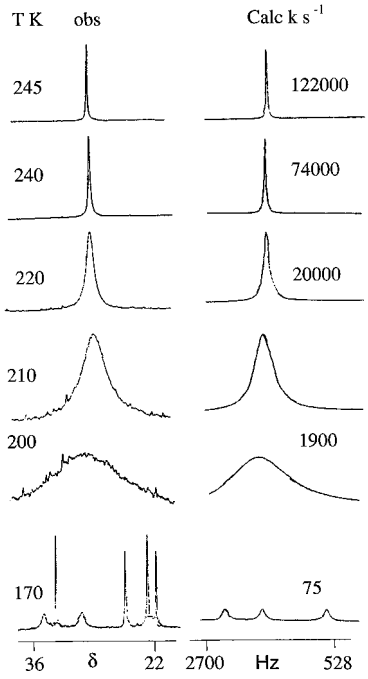

Figure 8. ^{13}C NMR compound **3** in diethyl ether, C-(CH_3)$_3$ part (left) observed at different temperatures and (right) calculated to fit with rate constants for rotation around the ring−*tert*-butyl bond.

to nuclear electric quadrupole-induced relaxation of ^{14}N.[11,12] The Hamiltonian (H), rotating frame, needed to ultimately plot the methyl ^{13}C line shape is given by (eq 7)

$$H = 2\pi\sum_{i}(\nu_i - \nu)I^{z}_{i} + 2\pi J\sum_{i} I^{z}_{i}I^{z}_{N} \qquad i = A, B, C \qquad (7)$$

where J is $^{1}J(^{13}C,^{14}N)$ and the other symbols are defined in Table 6. We use the spin product representation $\phi_C\phi_N$ to list the ^{13}C transitions of interest and abbreviate the states of ^{14}N by their

(10) Bushweller, C. H.; Anderson, W. G.; Stevenson, P. E.; Burkey, D. L.; O'Neil, J. W. *J. Am. Chem. Soc.* **1974**, *96*, 3892.

(11) Kaplan, J. I.; Fraenkel, G. *NMR in Chemically Exchanging Systems*; Academic Press: New York, 1980; Chapters 4 and 6.

(12) Fraenkel, G.; Subramanian, S.; Chow, A. *J. Am. Chem. Soc.* **1995**, *117*, 10336−10344.

$$R + K = \begin{bmatrix} -3r-2k & r & 2r & k & 0 & 0 & k & 0 & 0 \\ r & -2r-2k & r & 0 & k & 0 & 0 & k & 0 \\ 2r & r & -3r-2k & 0 & 0 & k & 0 & 0 & k \\ k & 0 & 0 & -3r-2k & r & 2r & k & 0 & 0 \\ 0 & k & 0 & r & -2r-2k & r & 0 & k & 0 \\ 0 & 0 & k & 2r & r & -3r-2k & 0 & 0 & k \\ k & 0 & 0 & -k & 0 & 0 & -3r-2k & r & 2r \\ 0 & k & 0 & 0 & k & 0 & r & -2r-2k & r \\ 0 & 0 & k & 0 & 0 & k & 2r & r & -3r-2k \end{bmatrix} \quad (11)$$

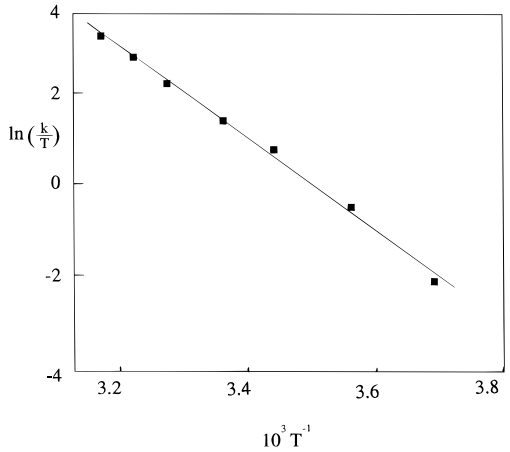

Figure 9. Eyring plot for inversion/rotation at the dimethylamino substituent in **4a** in CD_3NO_2.

Table 5. Activation Parameters from NMR Line Shape Analysis

compound	**4a**	**4a**	**4b**	**3**
anion	I^-	I^-	$CF_3SO_3^-$	
solvent	CD_3NO_2	acetone-d_6	acetone-d_6	Et_2O-d_{10}
inverting N				
$\Delta H^‡$ (kcal/mol)	18		17.3	16
$\Delta S^‡$ (eu)	17		14	17
rotation $X(CH_3)_3$				
$\Delta H^‡$		10.7	7.2	7.8
$\Delta S^‡$		5.5	−9	−3
^{14}N quadrupole relaxation E_a		2.7	2	

Table 6. Symbols Used in NMR Line Shape Calculations

$\Delta\nu_i = \nu - \nu_i$	R quadrupole relaxation operator
ν_i shift frequency	ρ^i density matrix
ν frequency axis	ρ^i(ae) density matrix after exchange
T^{-1} intrinsic line width	H spin Hamiltonian
k rate constant	C arbitrary weighting constant

m_z values (+1, 0, or −1) as $\alpha(+1) \rightarrow \beta(+1)$, $\alpha(0) \rightarrow \beta(0)$ and $\alpha(-1) \rightarrow \beta(-1)$. The required elements of the density matrix are $\rho^i_{\beta(+),\alpha(+)}$, $\rho^i_{\beta(0),\alpha(0)}$ and $\rho^i_{\beta(-1),\alpha(-1)}$ with i = A, B, and C and are abbreviated ρ^i_1, ρ^i_2, and ρ^i_3, respectively. In this system the ρ^i(ae) elements for rotation are obtained as before (eq 6), and we assume the spin state of ^{14}N does not change during a rotation of A → B. One takes all elements of the density matrix equation connected by a $\Delta m_z = 1$ ^{13}C

$$\langle\beta\phi_{Li}|\mathbf{i}[\rho^i,H] + (R - T^{-1})\rho + k(\rho^i(\text{ae}) - \rho^i)|\alpha\phi_{Li}\rangle = 0 \quad (8)$$

transition and diagonal in ^{14}N. This generates the set of nine coupled inhomogeneous equations in the ρ^i elements shown in matrix form as (eq 9),

$$[\mathbf{A} + \boldsymbol{T}^{-1} + \mathbf{R} + \boldsymbol{k}]\rho^i_{col} = -iC\mathbf{B}_{col} \quad (9)$$

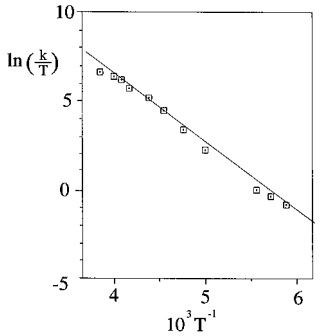

Figure 10. Eyring plot for rotation of the *tert*-butyl group in **3**.

in which $\mathbf{B}_{col}$ is a column of nine 1's, ρ^i_{col} is ρ^A_1, ρ^A_2, ρ^A_3, ρ^B_1, ρ^B_2, ρ^B_3, ρ^C_1, ρ^C_2, ρ^C_3. The elements of the diagonal A frequency matrix are shown in eqs 10a−10i and the remaining **R**+**K** matrix is shown in eq 11.

Elements of the quadrupole relaxation operator were obtained as described previously.[12,13] Since the extreme narrowing conditionis assumed to apply[11] only one relaxation parameter,

$$A_{1,1} = i2\pi(\Delta\nu_A - J) - T^{-1} \quad (10a)$$

$$A_{2,2} = i2\pi\Delta\nu_A - T^{-1} \quad (10b)$$

$$A_{3,3} = i2\pi(\Delta\nu_A + J) - T^{-1} \quad (10c)$$

$$A_{4,4} = i2\pi(\Delta\nu_B - J) - T^{-1} \quad (10d)$$

$$A_{5,5} = i2\pi\Delta\nu_B - T^{-1} \quad (10e)$$

$$A_{6,6} = i2\pi(\Delta\nu_B + J) - T^{-1} \quad (10f)$$

$$A_{7,7} = i2\pi(\Delta\nu_C - J) - T^{-1} \quad (10g)$$

$$A_{8,8} = i2\pi\Delta\nu_C - T^{-1} \quad (10h)$$

$$A_{9,9} = i2\pi(\Delta\nu_C + J) - T^{-1} \quad (10i)$$

r, is needed; it is defined in eq 12

$$r = 0.3\left(\frac{e^2qQ}{h}\right)^2\tau \quad (12)$$

wherein the term in parentheses is the quadrupole splitting constant and τ is the correlation time. As before, the absorption comes from the summation (eq 13).

$$\text{Abs} = -\text{Im}\sum_i(\rho^i{}_1 + \rho^i{}_2 + \rho^i{}_3)\text{A} \quad \text{i = A, B, C} \quad (13)$$

(13) Chow, A. M.S. Thesis, Ohio State University, Columbus, OH, 1982.

Since the ring−N^+ rotation and averaging of $^1J(^{13}C,^{14}N)$ effect the NMR over different temperature ranges, it was possible to first estimate the rates separately and then apply these values to the full line shape procedure described above. The resulting fitted, calculated line shapes (Figure 6) gave Eyring parameters $\Delta H^{\ddagger}$ and $\Delta S^{\ddagger}$ for rotation of respectively 10.7 kcal/mol and 5.5 eu (see Table 5). Regarding ^{14}N quadrupole-induced relaxation, we have plotted $1/r$ which gives E_a for τ^{-1}, or the correlation rate, of 2.7 kcal/mol (Table 5). The corresponding results for triflate **4b** in acetone-d_6 are similar to those for **4a** (see Table 5). Notice the similarity of the activation parameters for rotation of *tert*-butyl in **3** and of $N(CH_3)_3^+$ in **4a** and **4b**. This shows again the major influence of steric interactions in controlling dynamic processes in these systems.

All of the *cis*-2-substituted trimethylammonium species exhibit slow rotation around their ring−N^+ bonds at low temperature, as evidenced by separate ^{13}C peaks for the N^+ methyls or just broadening of the resonance. The latter is also the case for the *cis*-2-*tert*-butyltrimethylammonium salt **7** in acetone-d_6. By 200 K, the N^+ methyl resonance has broadened to a half width of 270 Hz. Below this temperature the compound crystallizes. It was not possible to prepare a cis vicinal di(trimethylammonium)-substituted cyclopentane to determine the extent to which steric interactions operated here also.

The *trans*-aminoammonium salts **5a** and **5b** exhibited only minor broadening of their respective N^+ methyl ^{13}C NMR resonances at low temperature, due possibly to the absence of major steric interactions. In contrast, the N^+ methyl ^{13}C NMR resonance of the trans vicinal di(quaternary ammonium)triflate **6**, which is narrow at room temperature, broadens on cooling and resolves by 200 K into two lines (2:1) at, respectively, δ 54.4 and δ 48.6. This behavior implicates slow rotation around the ring−N^+ bonds in **6** at low temperature.

In summary, the results presented here show the influence of steric interactions on dynamic processes in cis vicinal aminoammonium salts.

Experimental Section

General. Toluene and diethyl ether were distilled from sodium benzophenone ketyl prior to use. Titanium tetrachloride was stirred overnight with copper dust and then distilled under argon. Dimethylamine was condensed using a dry ice/acetone cold finger. Cyclopentane and pentane were distilled from sodium before use. All syringes were dried in an oven at 200 °C and then cooled under argon. The syringes used to transfer dimethylamine were first cooled in dry ice.

Equipment. NMR spectra were obtained using either a Brüker MSL 300 or AM 200 MHz Fourier transform NMR spectrometer.

[*cis*-2-(*N*,*N*-Dimethylamino)cyclopentyl]trimethylammonium Iodide (4a). Into a 250 mL round bottom flask containing a stir bar were introduced diethyl ether (100 mL) and *cis*-1,2-di(*N*,*N*-dimethylamino)cyclopentane (2.79 g, 0.0178 mol). Iodomethane (16 mL, 0.257 mol) was syringed into the flask with argon ebullition. A white solid formed, and the solution was stirred overnight. The powdery white solid was collected by vacuum filtration and then recrystallized from ethanol/isopropyl ether to give 2.00 g (0.0067 mol) of a sandy brown solid, [*cis*-2-(*N*,*N*-dimethylamino)cyclopentyl]trimethylammonium iodide, in 37.6% yield (mp 176−180 °C). ^1H NMR (D_2O) δ: 3.8−3.7 (m, 2H, CH), 3.34 (s, 9H, $N(CH_3)_3$), 2.29 (s, 6H, $N(CH_3)_2$), 2.35−1.6 (m, 6H, CH_2). ^{13}C NMR (D_2O) δ: 77.43 (CH−N^+), 66.20 (CH−N), 54.14 ($N(CH_3)_3$), 43.68 ($N(CH_3)_2$), 24.85 (CH_2), 21.72 (CH_2), 21.22 (CH_3).

[*cis*-2-(*N*,*N*-Dimethylamino)cyclopentyl]trimethylammonium Trifluoromethanesulfonate (Triflate) (4b). Into a 50 mL Schlenk flask with a stir bar were placed *cis*-1,2-di(*N*,*N*-dimethylamino)cyclopentane (2.04 g, 0.013 mol) and dichloromethane (15 mL) under argon. Methyl trifluoromethanesulfonate (2 mL, 0.018 mol) was syringed into the flask, and the solution was stirred overnight. The clear light brown solution was concentrated in vacuo to yield an oily brown liquid. The residue was recrystallized from isopropyl alcohol and petroleum ether to give 3.92 g (0.012 mol) of a white crystalline solid, [*cis*-2-(*N*,*N*-dimethylamino)cyclopentyl]trimethylammonium trifluoromethanesulfonate, in 94% yield. ^1H NMR (D_2O) δ: 3.09 (s, 9H, $N(CH_3)_3$), 2.04 (s, 6H, $N(CH_3)_2$), 1.9−1.4 (m, 6H, CH_2). ^{13}C NMR (D_2O) δ: 127.95 (CF_3), 122.85 (CF_3), 117.76 (CF_3), 112.67 (CF_3), 74.88 (CH−N^+), 64.12 (CH−N), 52.14 ($N(CH_3)_3$), 43.15 ($N(CH_3)_2$), 23.06 (CH_2), 19.95 (CH_2), 19.64 (CH_2).

[*cis*-2-(*N*,*N*-Dimethylamino)cyclopentyl]trimethylammonium Picrate (4c). In a 100 mL beaker containing boiling ethanol (60 mL) were combined [*cis*-2-(*N*,*N*-dimethylamino)cyclopentyl]trimethylammonium iodide (0.54 g, 0.0035 mol) and picric acid (0.56 g, 0.0025 mol). The solution turned red-brown and was cooled to room temperature. The oily red-brown solid which precipitated from the solution was left standing overnight, and a yellow crystalline solid formed. Ethanol was decanted from the solids. Recrystallization from acetone gave 0.5 g of a yellow-orange solid, [cis-2-(*N*,*N*-dimethylamino)cyclopentyl]trimethylammonium picrate, in 50% yield (mp 153−158 °C). ^{13}C NMR (acetone) δ: 126.16 (Ar), 76.75 (CH−N^+), 66.25 (CH−N), 53.73 ($N(CH_3)_3$), 24.09 (CH_2), 22.22 (CH_2), 20.49 (CH_2).

2-*tert*-Butylcyclopentanone (8). Into a 500 mL Schlenk flask containing dry dichloromethane (100 mL) at dry ice/acetone temperature were loaded by syringe, under argon, titanium tetrachloride (11 mL, 0.1 mol) and *tert*-butyl chloride (22 mL, 0.2 mol) in dichloromethane (50 mL). A green tinge appeared in the solution. (Trimethylsiloxy)-cyclopentene (15.63 mL, 0.1 mol) in dichloromethane (100 mL) was quickly added, and the solution turned black. After 1 h of stirring, the solution turned a dull green and a green solid precipitated. After 3 h of stirring, the solution was hydrolyzed with a saturated $NaHCO_3$ solution (40 mL). The mixture turned reddish and foamed. After 3 h of stirring at room temperature, the solution turned dark purple. It was then extracted with carbon tetrachloride (300 mL) and washed with a $NaHCO_3$ solution (3 × 100 mL) which turned the organic layer light yellow. The organic layer was dried overnight over Na_2SO_4 and then concentrated in vacuo to remove the carbon tetrachloride. The clear yellow residue was distilled under high vacuum to yield 5.77 g (0.041 mol) of a clear liquid, 2-*tert*-butylcyclopentanone (bp 80−84 °C at 4.5 Torr), in 41% yield. ^1H NMR ($CDCl_3$) δ: 2.13−1.14 (m, 7H, CH_2, CH), 0.88 (s, 9H, $C(CH_3)_3$). ^{13}C NMR ($CDCl_3$) δ: 212.69 (C═O), 57.72 (CH), 39.98 (CH_2), 32.21 (C−CH_3), 27.47 (CH_3), 26.14 (CH_2), 19.96 (CH_2).

***cis*-2-*tert*-Butyl-1-(*N*,*N*-dimethylamino)cyclopentane (3).** Into a 500 mL Schlenk flask equipped with a gas inlet and stir bar were introduced cyclopentane (300 mL) and 2-*tert*-butylcyclopentanone (5.77 g, 0.0412 mol) under argon. The flask was cooled to −78 °C with a dry ice/acetone bath. Dimethylamine (27 mL, 0.40 mol) was syringed into the flask. A 25 mL graduated cylinder was flame dried, cooled under argon and then fitted with a rubber septum. Cyclopentane (13 mL) and titanium tetrachloride (4.8 mL, 0.043 mol) were syringed into the cylinder and mixed. The clear solution was cannulated into the Schlenk flask, and an orange-red solid formed. After 3 h of stirring, the solution was warmed to room temperature and then stirred overnight under a positive pressure of argon.

The dark brown solution with a grayish-green solid was filtered through a layer of Celite and then a layer of Na_2SO_4 on a fritted glass funnel (50 mm, 1.45 μm). The solid was washed with cyclopentane (2 × 20 mL), and the dark brown solution was transferred to a flame-dried Parr jar, flushed with argon for 5 min, and then stoppered. The catalyst, 5% Pd on carbon (0.872 g), was quickly added, and the jar was placed on the hydrogenator. After flushing the solution with H_2 twice, the hydrogenator was charged with 65 psi of H_2 and shaken for 2 days. The solution was filtered through Celite to remove the catalyst and then concentrated in vacuo to remove the cyclopentane. The remaining liquid was distilled under reduced pressure to yield 4.27 g (0.025 mol) of a light yellow liquid, *cis*-2-*tert*-butyl-1-(*N*,*N*-dimethylamino)cyclopentane (bp 52−57 °C at 2.7 Torr), in 61.36% yield. ^1H NMR ($CDCl_3$) δ: 2.97 (t, 1H, CH−N), 2.08 (s, 6H, $N(CH_3)_2$), 2.0−1.82 (m, 4H, CH), 1.70−1.60 (m, 2H, CH_2), 1.55−1.3 (m, 2H, CH_2), 1.00 (s, 9H, $C(CH_3)_3$). ^{13}C NMR ($CDCl_3$) δ: 67.08 (CH−N), 55.77 (CH−C), 43.56 ($N(CH_3)_2$), 32.03 (C−CH_3), 28.91 ((CH_3)$_3$), 25.64 (CH_2), 23.07 (CH_2), 22.50 (CH_2).

(*cis*-2-*tert*-Butylcyclopentyl)trimethylammonium Trifluoromethanesulfonate (7). A 25 mL round bottom flask was charged with *cis*-2-

tert-butyl-1-(*N*,*N*-dimethylamino)cyclopentane (0.845 g, 0.005 mol) in dichloromethane (15 mL) under argon. Methyl trifluoromethanesulfonate (0.6 mL, 0.005 mol) was added via syringe, and the solution was stirred overnight under a positive pressure of argon. The solution was concentrated in vacuo to remove the dichloromethane yielding an orange-red solid. The latter was recrystallized from ethanol/petroleum ether to give 0.845 g (0.0026 mol) of white crystals, (*cis*-2-*tert*-butylcyclopentyl)trimethylammonium trifluoromethanesulfonate (mp 100−104 °C), in 52% yield. ^{1}H NMR (D_2O) δ: 3.94 (q, 2H, CH), 3.18 (s, 6H, $N(CH_3)_3$), 2.1−1.6 (m, 6H, CH_2) 1.07 (s, 9H, $C(CH_3)_3$). ^{13}C NMR (D_2O) δ: 120.55 (CF_3, $^1J(^{13}C,^{19}F) = 318.1$ Hz), 80.23 (CH−N), 56.21 (CH−$C(CH_3)$), 53.92 ($N(CH_3)_3$), 32.61 ($C-CH_3$), 30.46 ($(CH_3)_3$), 26.60 (CH_2), 25.38 (CH_2), 19.98 (CH_2).

***trans*-*N*,*N*,*N*′,*N*′-Tetramethylcyclopentane-1,2-diamine (2).** A 250 mL round bottom flask equipped with a condenser and stir bar was charged with *trans*-1,2-cyclopentadiammonium dichloride (12.25 g, 0.0708 mol), formic acid (50 mL, 1.30 mol, 90%), and formaldehyde (50 mL, 1.80 mol, 40%). The solution was heated to 90 °C, and bubbling was observed. After the bubbling stopped, the solution was heated to 95 °C and stirred overnight. The brown solution was cooled to room temperature and made basic (pH = 11) with solid KOH. The solution was extracted with diethyl ether (5 × 100 mL) and then with chloroform (5 × 100 mL). The extracts were combined, dried over $MgSO_4$, and then concentrated in vacuo. The brown oil was distilled under high vacuum to yield 5.53 g (0.0354 mol) of a clear liquid, *trans*-*N*,*N*,*N*′,*N*′-tetramethylcyclopentane-1,2-diamine (bp 98−103 °C at 65 Torr), in 50% yield. ^{1}H NMR (CDCl33) δ: 2.48 (m, 2H, CH), 2.00 (s, 12H, $N(CH_3)_2$), 1.33 (m, 6H, CH_2). ^{13}C NMR ($CDCl_3$) δ: 68.48 (CH), 42.05 ($N(CH_3)_2$), 24.85 (CH_2), 23.21 (CH_2).

[*trans*-2-(*N*,*N*-Dimethylamino)cyclopentyl]trimethylammonium Iodide (5a). Diethyl ether (100 mL) and *trans*-*N*,*N*,*N*′,*N*′-tetramethylcyclopentane-1,2-diamine (1 g, 0.0064 mol) were introduced into a 250 mL round bottom flask with a stir bar. Iodomethane (3 mL, 0.048 mol) was syringed into the flask, and argon was bubbled through the solution. A white solid formed, and the solution was stirred overnight. A powdery white solid was collected by vacuum filtration and was recrystallized from ethanol/isopropyl ether to give 1 g (0.0034 mol) of the title compound as a yellow white solid (mp 202−206 °C) in 53% yield. ^{1}H NMR (CD_3NO_2) δ: 4.0−3.8 (m, 2H, CH), 3.2 (s, 9H, $N(CH_3)_3$), 2.3 (s, 6H, $N(CH_3)_2$), 2.2−1.6 (m, 6H, CH_2). ^{13}C NMR (CD_3NO_2) δ: 77.64 (CH−N^+)), 66.28 (CH−N), 52.74 ($N(CH_3)_3$), 40.90 ($N(CH_3)_3$), 26.60 (CH_2), 22.69 (CH_2), 20.66 (CH_2).

***trans*-Cyclopentyl-1,2-di(trimethylammonium) Di(trifluoromethanesulfonate) (6).** The reaction vessel, a 50 mL Schlenk flask with a stir bar, was loaded with *trans*-*N*,*N*,*N*′,*N*′-tetramethylcyclopentane-1,2-diamine (0.8 g, 0.0051 mol) and dichloromethane (15 mL) under argon. Methyl trifluoromethanesulfonate (2 mL, 0.018 mol) was syringed into the flask, and the solution was stirred overnight. The clear light brown solution was concentrated in vacuo to yield an oily brown liquid. The latter was recrystallized from isopropyl alcohol/petroleum ether and placed under vacuum overnight to give 1.10 g (0.0023 mol) of a light brown powdery solid, *trans*-cyclopentyl-1,2-di(trimethylammonium) di(trifluoromethanesulfonate) (mp 118−120 °C), in 44% yield. ^{1}H NMR (acdetone) δ: 5.0 (d, 2H, CH), 3.4 (s, 18H, $N(CH_3)_3$), 2.8−2.4 (m, 4H, CH_2), 2.2−2.1 (p, 2H, CH_2). ^{13}C NMR (acetone) δ: 75.89 (CH−N), 53.50 ($N(CH_3)_3$), 28.21 (CH_2), 25.45 (CH_2).

Acknowledgment. This research was generously supported by the National Science Foundation Grant NO CHE-9317298 as was also, in part, the purchase of NMR equipment used in this research. We are happy to acknowledge expert technical help and advice from Dr. Charles Cottrell, Central Campus Instrumentation Center, The Ohio State University.

Supporting Information Available: X-ray crystallographic details and additional Eyring plots (22 pages). See any current masthead page for ordering and Internet access instructions.

JA962327Z